5

MgB_2-MgO Compound Superconductor

Yi Bing Zhang and Shi Ping Zhou
Department of Physics, College of Science, Shanghai University, Shanghai 200444 China

1. Introduction

1.1 Superconductive materials

Since the first superconductor, mercury (Hg), was discovered in 1911 by H. Kamerlingh Onnes and his students, there are thousands of superconducting materials were reported up to now. By 1980 superconductivity had been observed in many metals and alloys. Most metals in the periodic table exhibit superconductivity, aside from the ferromagnetic transition metals and rare-earth and actinide metals. Several nonsuperconducting elements will also have a superconductive state under high pressure. Niobium (Nb) has the highest T_c (9.2 K) among all elements at normal pressure. The A-15 compound Nb_3Ge remained the highest transition temperature (T_c = 23.2 K) until the high-T_c cuprate superconductors discovered by Bednorz and Müller (Bednorz & Müller, 1986) in 1986.

The cuprate superconductors adopt a perovskite structure and are considered to be quasi-two dimensional materials with their superconducting properties determined by electrons moving within weakly coupled copper-oxide (CuO_2) layers. There are several families of cuprate superconductors, including $YBa_2Cu_3O_{7-\delta}$, $Bi_2Sr_2Ca_nCu_{n+1}O_{6+2n+\delta}$, $Tl_mBa_2Ca_nCu_{n+1}O_{4+m+2n+\delta}$ (m = 1, 2), $HgBa_2Ca_nCu_{n+1}O_{4+2n+\delta}$ etc., where n may be 0, 1, and 2. They raise T_c of superconductor to 92 K, 110 K, 125 K, and 135 K respectively. Usually, they are categorized by the elements that they contain and the number of adjacent copper-oxide layers in each superconducting block. For example, YBCO and BSCCO can alternatively be referred to as Y123 and Bi2201/Bi2212/Bi2223 depending on the number of layers in each superconducting block (L). The superconducting transition temperature has been found to peak at an optimal doping value (p = 0.16) and an optimal number of layers in each superconducting block, typically L = 3. The weak isotope effects observed for most cuprates contrast with conventional superconductors that are well described by BCS theory. Another difference of the high-temperature superconducting oxides from the conventional superconductors is the presence of a pseudo-gap phase up to the optimal doping.

The first superconducting oxide without copper element is an iron-based superconductor, LaFeOP, which was discovered in 2006 by Y. Kamihara et al. (Kamihara et al., 2006) at Tokyo Institute of Technology, Japan. It is gained much greater attention in 2008 after the analogous material LaFeAs(O,F) was found with superconductivity at 43 K (Kamihara et al., 2008; Takahashi et al., 2008) under pressure. Within just a few months, physicists in China found optimal electron and hole dopants then doubled T_c to 55 K (Ren et al., 2008). The iron-based superconductors contain layers of iron and a pnictogen such as arsenic or phosphorus, or chalcogens. This is currently the family with the second highest critical

temperature, behind the cuprates. Since the original discoveries, two main families of iron-based superconductors have emerged: the rare-earth (R) iron-based oxide systems $RO_{1-x}F_xFeAs$ (R = rare earth) and the $(Ca,Ba,Sr)_{1-x}KxFe_2As_2$. Most undoped iron-based superconductors show a tetragonal-orthorhombic structural phase transition followed at lower temperature by magnetic ordering, similar to the cuprate superconductors. However, they are poor metals rather than Mott insulators and have five bands at the Fermi surface rather than one. Strong evidence that the T_c value varies with the As-Fe-As bond angles has already emerged and shows that the optimal T_c value is obtained with undistorted FeAs tetrahedra.

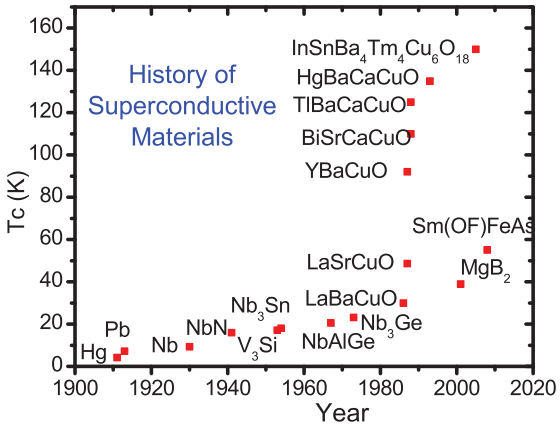

Fig. 1. Survey diagram for superconductive materials. $InSnBa_4Tm_4Cu_6O_{18+}$ is a multiphase superconductor with a possible superconductivity at 150 K (Patent No.: US60/809,267) and T_c of this family is up to about 250 K in 2010.

Fig. 1 shows the survey of superconductive materials. Other potential superconducting systems with a high transition temperature may also include fulleride superconductors, organic superconductors, and heavy fermion compounds. Theoretical work by Neil Ashcroft (Ashcroft, 1968) predicted that liquid metallic hydrogen at extremely high pressure should become superconducting at approximately room-temperature because of its extremely high speed of sound and expected strong coupling between the conduction electrons and the lattice vibrations. Scientists dream to find room-temperature superconductors but the survey of discovering superconductors indicates that only 1 ~ 2 K of T_c was increased per year from the first element superconductor to the first high- T_c cuprate oxide and after the discovery of TlBaCaCuO to now.

Even though new superconductive families and new T_c value are reported in the cuprate oxides, their structures become more and more complicated. Scientists expect new superconductors with simple structure for theory studying and device fabricating and well mechanic behavior for application. But the history stepping of superconductor discoveries seems to have its rule. In 2001 the discovery of superconductivity in magnesium diboride (Nagamatsu et al., 2001), a simple compound with only two elements and well metallic behavior, excite scientists again for studying alloy superconductors. It also opens an attractive application in the high power and superconductive electronics due to its transition

temperature (~ 40 K) far above liquid Helium, high critical current density (10^6 ~ 10^7 A/cm^2 at low temperatures and zero field), larger coherence length (ξ ~ 3 ~ 12 nm) than high temperature superconductors (HTSC), and the characteristic of transparent grain boundaries. Funnily, this compound had been synthesized in 1950s but its superconductivity was discovered until 2001. Fig. 2 shows the history diagram of discovering conventional superconductors, in which the points distribute closely along the fitting curve. Therefore it may be not surprising that the superconductivity of MgB_2 was disclosed until 2001 and superconductors with a transition temperature above liquid nitrogen boiling point may be found after 2060.

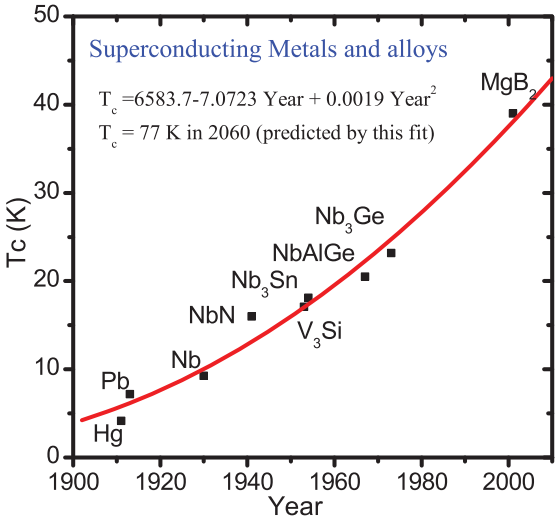

Fig. 2. The date dependence of critical temperature (T_c) for conventional superconductors.

1.2 Compound superconductors

Mixing one of superconductors mentioned above with other materials, we may obtain superconducting composite. Superconducting-nonsuperconducting composites or some granular superconducting materials with weak-link characteristics can be regarded as those composed of superconducting grains embedded in a non-superconducting host. The latter can be a normal metal, an insulator, a ferromagnet, a semiconductor, or a superconductor with lower transition temperature. Several reports suggested that these materials may exhibit novel properties (Shih et al., 1984; John & Lunbensky, 1985; Petrov et al., 1999; John & Lunbensky, 1986; Gillijns et al., 2007) different from their pure superconducting phases and be useful in practical applications. One striking feature of such materials is the existence of two superconductive transitions: a higher one at which the grains become superconducting but the matrix remains normal and a lower one at which the whole composite becomes superconducting but the critical current density is low. Another attractive feature is that the magnetic flux pinning and critical current density of superconducting composites are enhanced (Matsumoto et al., 1994; li Huang et al., 1996) at a low fraction of several non-superconductors. The most obvious application of these

materials is to make a superconducting fault current limiter (SFCL) because composite superconductors have a broad range of current-carrying capacity (Mamalis et al., 2001).
The superconducting material, MgB_2, which superconductivity at 39 K was discovered in 2001 by Akimitsu's group (Nagamatsu et al., 2001), has shown a huge potentiality of theory researches and applications for high-performance electronic devices and high-energy systems (Xi, 2008). Scientists believe that it will be the best material, up to now, to replace the traditional niobium (Nb) and Nb alloy superconductors working at the liquid helium temperature. Comparing with high-temperature superconducting oxides (HTSC), the glaring properties of MgB_2 include transparent boundaries without weak links (Larbalestier et al., 2001; Kambara et al., 2001), high carrier density, high energy gaps, high upper critical field, low mass density, low resistivity (Xi et al., 2007), and low anisotropy (Buzea & Yamashita, 2001). Owing to the strong links among MgB_2 grains, there is no much influence on its superconductivity when a sample was contaminated or doped by a small ratio. Experimental results reported by Wang's group (Wang et al., 2004) and Ma's group (Ma et al., 2006; Gao et al., 2008) showed that the critical current density and flux pinning in some doping were enhanced evidently. Several papers suggested also that there was no appreciable difference between a perfect MgB_2 sample and one with MgO or oxygen contamination, but the flux pinning was improved (Eom et al., 2001; Przybylski et al., 2003; Zeng et al., 2001; Liao et al., 2003). These characteristics interest us in studying compound MgB_2 superconductor. Mitsuta et al. (Matsuda et al., 2008) reported the properties of MgB_2/Al composite material with low and high fraction of MgB_2 particles and Siemons et al. (Siemons et al., 2008) demonstrated a disordered superconductor in MgB_2/MgO superstructures. But there are little data for superconducting MgB_2 composites when the content of non-superconducting phase is comparable to or even more than one of MgB_2 phase.

2. The synthesis and superconductivity of MgB_2-MgO compound superconductor

2.1 Structure, fabrication and physical properties of MgB_2

MgB_2 has a very simple AlB_2-type crystal structure, hexagonal symmetry (space group P6/mmm) with unit cell lattice parameters a = 3.08136(14) Å and c = 3.51782(17) Å, where the boron atoms form graphite-like sheets separated by hexagonal layers of Mg atoms. The magnesium atoms are located at the centre of hexagons formed by borons and donate their electrons to the boron planes. Similar to graphite, MgB_2 exhibits a strong anisotropy in the B-B lengths: the distance between the boron planes is significantly longer than the inplane B-B distance.
Magnesium diboride can be synthesized by a general solid phase reaction, by using boron and magnesium powders as the raw materials. However, there are two main problems to block the path for obtaining a high-quality MgB_2 superconducting material. Firstly, magnesium (Mg) has very high vapor pressure even below its melting point. Meanwhile there is a significant difference in the melting points between Mg and B (Mg: 651 ˚C and B: 2076 ˚C). Secondly, Mg is sensitive to oxygen and has a high oxidization tendency. On the other hand, the thermal decomposition at high temperature is also a problem in the synthesis of MgB_2. So a typical method is to wrap the samples with a metal foil, for example Ta, Nb, W, Mo, Hf, V, Fe etc., then sinter by high temperature and high Ar pressure.

Superconducting magnesium diboride wires are usually produced through the powder-in-tube (PIT) process.

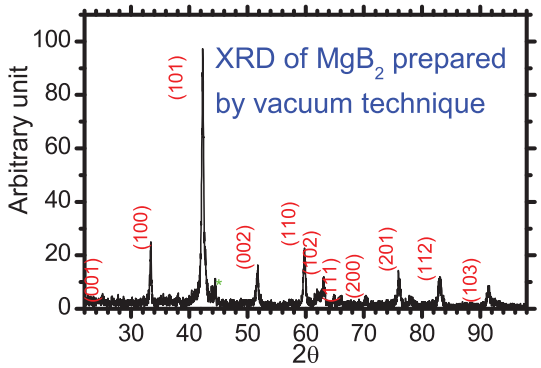

Fig. 3. X-ray diffraction pattern of superconducting MgB_2 sample synthesized by the vacuum technique.

Several reports showed that MgB_2 can be prepared by vacuum techniques rather than high-pressure atmosphere and metal wrapping. Fig. 3 shows the X-ray diffraction pattern of a superconducting MgB_2 sample synthesized by the vacuum technique in the authors' laboratory. It indicates that no MgO or other higher borides of magnesium (MgB_4, MgB_6, and MgB_{12}) are detected excluding the phase of MgB_2. Magnesium and boron powder were mixed at the mole ratio of Mg : B = 1 : 2, milled, pressed into pellets, then sintered in a vacuum furnace at about 5 Pa and 800 ˚C for 2 hours. The temperature dependence of resistance of the sample in the vicinity of transition temperature is shown in Fig. 4. The sample has well metallic behavior with a high transition temperature (39.2 K) and narrow transition width (0.3 K), a residual resistance ratio, RRR = R(300 K)/R(40 K) = 3.0, resistivity at 300 K estimated about 110 μΩ, and critical current density higher than 10^6 A /cm² at 5 K and zero field. These results indicate that high-quality superconducting MgB_2 bulks can be fabricated by the vacuum route. Comparing with high-temperature cuprate oxides and conventional superconductors, magnesium diboride exhibits several features listed below:

a. Highly critical temperature, T_c = 39 K, out of the limit of BCS theory.
b. High current carrier density: 1.7 ~ 2.8 × 10^{23} holes/cm^3, a value that is 2 orders higher than ones of YBCO and Nb_3Sn.
c. High and multiple energy gaps, $2\Delta_1$ = 17 ~ 19 meV, $2\Delta_2$ = 7 ~ 9 meV.
d. Highly critical current density, J_c (4.2 K, 0 T) > 10^7 A/cm^2.
e. Larger coherent lengths than HTSC, $\xi_{ab}(0)$ = 37 ~ 120 Å, $\xi_c(0)$ = 16 ~ 36 Å.
f. High Debye temperature, Θ_D ~ 900 K.
g. Negative pressure effect, dT_c/dp = – 1.1 ~ 2 K/GPa.
h. Positive Hall coefficient.
i. Very low resistivity at normal state.

These characteristics indicate that MgB_2 has the potentiality of superconductive applications in high-power field and electronic devices and will be the best material to replace the traditional niobium (Nb) and Nb alloy superconductors working at the liquid helium temperature.

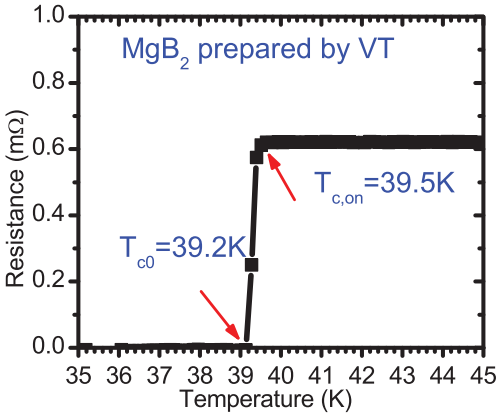

Fig. 4. The temperature dependence of resistance of superconducting MgB_2 sample synthesized by the vacuum technique in the vicinity of transition temperature.

2.2 Preparation of MgB_2-MgO compound superconductor

(Zhang et al., 2009)

Magnesium oxide (MgO) has the cubic crystal structure with a lattice parameter a=4.123 Å, which is close to one of MgB_2. Considering that MgO phase is easily to be formed in the process of preparing MgB_2 superconductor and a small amount of MgO contamination will not degrade evidently the superconductivity of MgB_2, the authors are interested in studying MgB_2-MgO Compounds. The superconducting MgB_2-MgO composite with about 75% mole concentration of MgO was synthesized *in situ* by a single-replacement reaction.

The magnesium powder (99% purity, 100 mesh) and B_2O_3 (99% purity, 60 mesh) were mixed at the mole ratio of Mg: B_2O_3=4:1, milled, and pressed into pellets with a diameter of 15 mm and thickness of 5 ~ 10 mm under a pressure of 100 MPa. These pellets were placed in a corundum crucible which was closed by an inner corundum cover, and then fired in a vacuum furnace by the sequential steps: pumping the vacuum chamber to 5 Pa, heating from room temperature to 400 °C and holding 2 hours, increasing temperature by a rate of greater than 5 °C/min to 600 °C and holding about 1 hour, then 800 °C × 1 hour for completing reaction, and, finally, cooling naturally to room temperature. A more detail of the synthesis processes can be found in China Patent No. ZL 200410017952.0, on July 19, 2006. That holding 2 hours at 400 °C was to vitrify B_2O_3 completely at a low temperature and 1 hour at 600 °C was to diffuse and mix Mg sufficiently with B_2O_3 below the melting point of magnesium. The furnace pressure was maintained at a value of lower than 5 Pa by a vacuum pump while sintering. The sample preparation can be described by a solid-state replacement reaction as follows:

$$4Mg + B_2O_3 = MgB_2 + 3MgO \quad (1)$$

The raw materials, Mg and B_2O_3, are available commercially and B_2O_3 powder is far cheaper than B. The small difference of melting points between Mg and B_2O_3 allows the sample synthesis without high pressure. The moderate reaction condition and the low-cost starting materials used in this method are favorable for practical application.

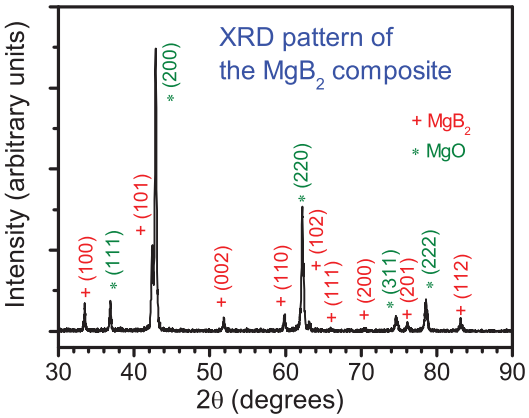

Fig. 5. X-ray diffraction pattern of superconducting MgB_2-MgO composite. Only diffraction peaks of MgB_2 and MgO phases were detected. The mass ratio of MgB_2 to MgO in the sample was calculated to 1:2.6.

The x-ray powder diffraction (XRD) pattern, as shown in Fig. 5, measured by Rigaku/D Max2000 x-ray diffractometer confirmed that only MgB_2 and MgO phases were detected in the composite and the mass ratio of MgB_2 to MgO was calculated to 1:2.6. Thus the mole fractions of MgB_2 and MgO in the composite were roughly 25% and 75% respectively. It means that the replacement reaction mentioned above was realized and complete. The samples exhibited black color, soft texture, and low density. The measured mass density was in the range of 1.4 ~ 2.3 g/cm^3, which is lower than the theoretical density, 2.625 g/cm^3 for MgB_2 and 3.585 g/cm^3 for MgO. The lattice parameters of MgB_2 calculated by XRD were a=3.0879 A° and c=3.5233 Å, which are consistent with ones of a pure MgB_2 sample.
The SEM image of the MgB_2-MgO sample at 15.0 kV and a magnification of 50,000 is shown in Fig. 6. The MgB_2 crystal grains, embedded dispersedly in MgO matrix, with a size of 100 ~300 nm can be observed obviously. MgO grains with a far smaller size than MgB_2 are filled in the boundaries and gaps among MgB_2 crystal grains. Such crystallite size and distribution indicate this is an ideal composite for studying the boundary and grain connection properties of MgB_2 superconductor.

2.3 Superconductivity in MgB_2 -MgO composite

(Zhang et al., 2009; 2010)
The resistance of the composite as a function of temperature was measured from 10 K to 300 K by the standard four-probe method in a close-cycle refrigeration system. Fig. 7 shows that the temperature dependence of resistance of the superconducting MgB_2-MgO composite and the pure MgB_2 bulk fabricated by the general solid reaction and vacuum sintering techniques. Comparing with the pure MgB_2 bulk, it is scientifically interesting that the composite exhibited an excellently electrical transport behavior and a narrow normal superconductive (N-S) transition. The onset transition temperature ($T_{c,on}$) and the critical transition temperature (T_c, at 50% of the onset transition resistance) were 38.0 K and 37.0 K respectively. The transition temperature width ΔT_c, which was calculated from 90% to 10%

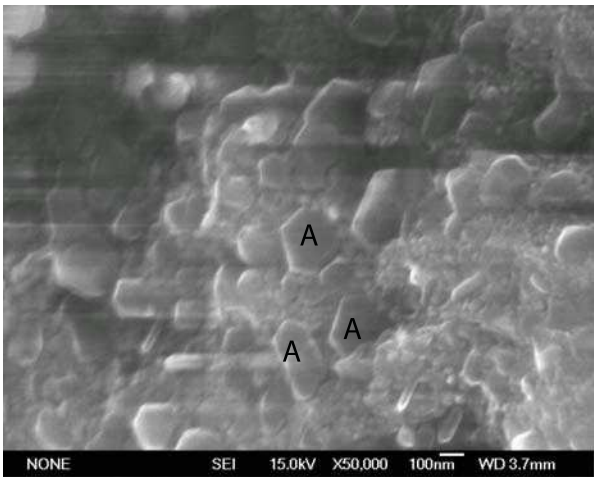

Fig. 6. (Zhang et al., 2009) Image of scanning electronic microscopy (SEM) of the superconducting MgB_2-MgO composite. Examples of MgB_2 crystal grains were labelled by the letter "A".

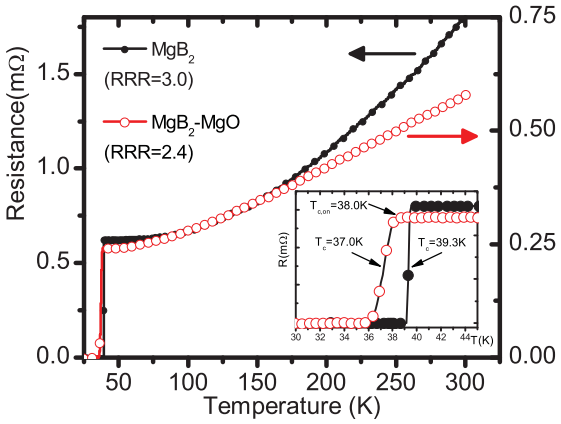

Fig. 7. (Zhang et al., 2010) Resistance vs temperature (R-T) curves of superconducting MgB_2-MgO composite and pure MgB_2 bulk. The inset shows their R-T curves in the vicinity of N-S transition.

of the onset transition resistance, was only 0.6 K. The residual resistance ratio, RRR=R(300 K)/R(40K), was 2.4, which was also comparable to the value (RRR=3.0) of our pure MgB_2 bulk samples.

Most experimental results showed that the transition temperature T_c of MgB_2 has weak dependence with the RRR value or high resistivity at normal state (Rowell, 2003), and the resistivity dependence with temperature at normal state can be pictured by the following formula.

$$\rho = \rho_0 + AT^n \quad (2)$$

The exponent n was measured to be 3 for a single crystal sample and ranged from 2 to 3 for the multicrystal. These R-T behaviors of MgB_2 at normal state may be explained by using the two-band model and considering π-band and σ-band contributions (Varshney, 2006). For our samples of pure MgB_2 multicrystal, the above formula is a good R-T expression and the exponent n was fitted to 2.3. But for the superconducting MgB_2-MgO composite, it seems not to be a proper approximation.

Zero resistance, which will be detected when continuous carrier's paths exist in a sample, may not mean the bulk superconducting characteristics. In Fig. 8, the temperature dependence of the real part (χ') and the imaginary one (χ'') of ac magnetic susceptibility is given at an ac field amplitude of 10 Oe and frequency of 777 Hz. It shows a diamagnetic transition at 37 K with a broad transition width. The imaginary part has a positive peak at 32 K and the saturation is observed at about 20 K. The diamagnetic transition at the temperature of 37 K is consistent with the R-T result. It means that the MgB_2-MgO composite is a bulk superconductor. Therefore, the composite may be utilized as a bulk superconductor or applied in superconductive function devices. One possible application is to make the superconducting fault current limiter (SFCL) because MgO has no obvious influence on the superconductivity of MgB_2 as well as the absence of chemical reaction between them. Composite superconductors have broad current carry and are considered the best material of SFCL (Mamalis et al., 2001). In addition, the composite implies a new potentiality of preparing MgB_2 superconductor when MgO is removed by some effective methods, for example, chemical wash or high-voltage static separation.

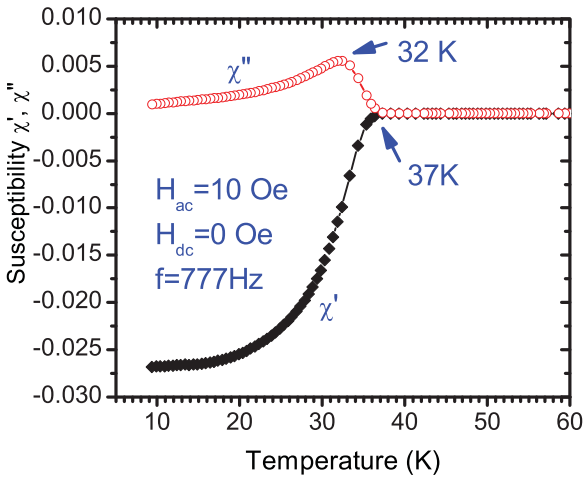

Fig. 8. Temperature dependence of the real component (χ') and the imaginary one (χ'') of ac magnetic susceptibility at the ac field amplitude 10 Oe and frequency 777 Hz. The magnitude of susceptibility was not normalized in this figure (Zhang et al., 2009).

3. Electric transport characteristics of MgB_2-MgO composite

(Zhang et al., 2009; 2010)

3.1 Effective media and statistical percolation theories

MgO is an insulator and MgB_2 is a good conductor with low resistivity. The conductivity of MgB_2-MgO composite belongs to a metal-insulator transport problem. A metal-insulator conductance is generally pictured by effective media theories (EMT) (Nan, 1993) or percolation theories (PT) (Lux, 1993; Kirkpatrick, 1973). There are the following four typical expressions, symmetric Bruggeman (SB) approximation of EMT, Clausius-Mossotti (CM) function of EMT, statistical percolation (SP) model, and McLachlan (ML) phenomenological equation (McLachlan et al., 2003) to explain the electrical conductivity (σ_m) of a metal-insulator mixture.

$$\begin{cases} \sigma_m^{SB} = \frac{1}{2}[(3\phi-1)\sigma_i], & \phi > \frac{1}{3}, & \text{SBapprox.} \\ \sigma_m^{CM} = \frac{2\phi}{3-\phi}\sigma_i, & \phi >= 0, & \text{CMapprox.} \\ \sigma_m^{SP} = \sigma_i(\phi-\phi_c)^{\mu}, & \mu = 1.7 \sim 1.9, & \text{SPmodel} \\ \sigma_m^{ML} = \sigma_i\frac{(\phi-\phi_c)^t}{(1-\phi_c)^t}, & t = 1.5 \sim 3.1, & \text{MLequation} \end{cases}$$

Here ϕ is the volume fraction of the metal phase, ϕ_c is the critical volume fraction with a value of 0.16 ± 0.02 in the 3D lattice site percolation model (Zallen, 1983), σ_i is the electric conductivity of the metal phase, μ and t are critical exponents. Fig. 9 shows normalized conductivities of a metal-insulator composite as a function of volume fraction calculated by SB, CM, SP, and ML approximations. The inset gives the measured conductivity of W-Al_2O_3 composite (Abeles et al., 1975), and fitted data by the SP estimation and ML approximation. At a low volume fraction of the metal phase, the SP model gives the best explanation for the conductivity of a metal-insulator mixture. The effective media theories can only give qualitative results, owing to its simplicity. When the host phase is an insulator, McLachlan (ML) phenomenological equation shows accordant results with the statistical percolation (SP) model at low (ϕ–ϕ_c). In fact, ML conductivity function may be understood as the normalization expression of SP model.

3.2 Conductivity vs. temperature of MgB_2 composite

The electrical transport behavior of a metal-insulator composite can be described well by the statistical percolation model. But, as we know that the percolation model is a pure geometrical problem, it can not give a conductivity expression with temperature. However, if the temperature dependence of volume fraction, (ϕ–ϕ_c), could be obtained, we believe that SP model shall still be an simple and practical approach to understand the electrical transport behavior of a metal-insulator composite.

Thermal expansion measurements indicated that lattice parameters of MgB_2 have strong dependence on temperature, $\alpha_a \approx 5.4 \times 10^{-6}\,K^{-1}$, $\alpha_c \approx 11.4 \times 10^{-6}\,K^{-1}$, and $\alpha \approx 8 \times 10^{-6}\,K^{-1}$ for a multicrystal sample (Lortz et al., 2003; Jorgensen et al., 2001; Neumeier et al., 2005). It will result in the temperature dependence of (ϕ– ϕ_c) and then influence on the conductivity of

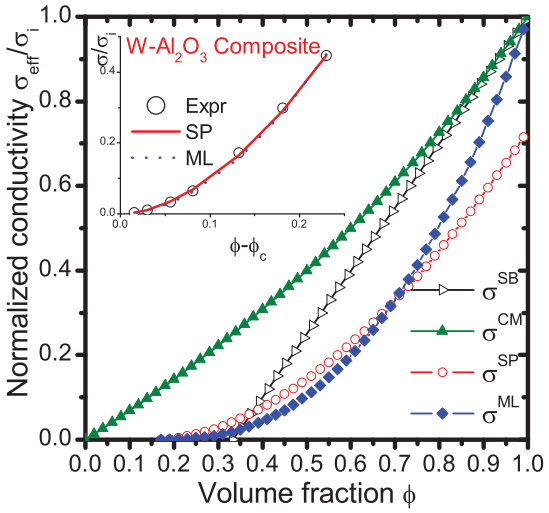

Fig. 9. The volume fraction dependence of composite's conductivity calculated by SB, CM, SP, and ML approximations. The inset shows the normalized conductivity of W-Al_2O_3 composite: "○" refers to the experimental data (Abeles et al., 1975), "—" SP result at μ=1.8, "…" ML approximation at t=1.8.

the metal-insulator mixture. According to measured mass density and the scanning electron microscope (SEM) image of the composite (Zhang et al., 2009), we noticed that the composite is not dense and the host phase is an insulator (MgO) with crystal grain sizes of far smaller than ones of the metal phase (MgB_2). Both of MgO particles and the holes in the composite can be regarded as an insulating background for superconducting MgB_2 grains to embed. The grain size variation of MgO is neglected and the grain size variation of MgB_2 with temperature has no influence on the whole volume of mixture. Thus a model of the temperature dependence of composite volume fraction is proposed and shown in Fig.10. Suppose V is the total volume of mixture, r_{i0} and $r_i(T)$ are the i^{th} grain's radius of MgB_2 at temperature 0 K and T K respectively.

Supposing all MgB_2 grains are spherical for simplifying calculation, then the volume fractions of metal phase at 0 K and T K are:

$$\phi_0 = \phi(0) = \frac{1}{V}\sum(\frac{4}{3}\pi r_{i0}^3); T = 0K \tag{3}$$

$$\phi = \phi(T) = \frac{1}{V}\sum_i(\frac{4}{3}\pi r_i^3(T)) \tag{4}$$

Grain radiuses of conductive phase satisfy with the normal distribution law.

$$n(r) = \frac{1}{r\sqrt{2\pi}\delta}\exp\left(-\left[\frac{\ln(r/r_0)}{\sqrt{2}\delta}\right]^2\right) \tag{5}$$

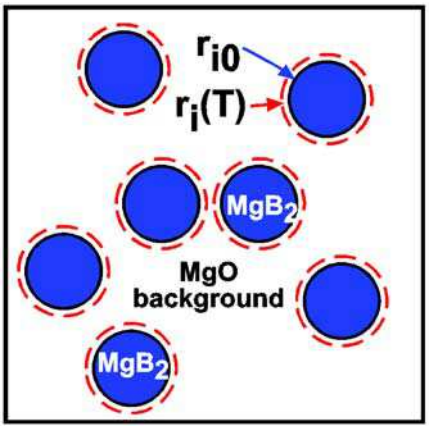

Fig. 10. Diagram of a simple model for the temperature dependence of composite volume fraction (Zhang et al., 2010).

Here r is the effective grain radius, r_0 is the effective mean radius, and δ is the standard deviation. Hence, the volume fraction can be calculated by the average radius: r_0 at 0 K and r at T K. Assume the grain number of the conductive phase is N and the grain number per volume is n, then

$$\phi_0 = \phi(0) = \frac{N}{V}\frac{4}{3}\pi r_0^3 = \frac{4}{3}n\pi r_0^3 \tag{6}$$

$$\phi = \phi(T) = \frac{N}{V}\frac{4}{3}\pi r^3(T) = \frac{4}{3}n\pi r^3(T) \tag{7}$$

The thermal expansion coefficient of MgB_2 satisfies well with Grüneisen relationship (Neumeier et al., 2005; Jorgensen et al., 2001; Xue et al., 2005):

$$\beta = 3\alpha = \gamma_G \kappa_T C_V / V \tag{8}$$

Where β is the volume expansivity of MgB_2, α is its linear expansivity, γ_G Grüneisen constant, κ_T isothermal compressibility and almost independence with temperature, C_V specific heat at constant volume. Specific heat C_V of MgB_2 at normal state as a function of temperature can be written as:

$$C_V = \gamma T + \beta_3 T^3 + \beta_5 T^5 \tag{9}$$

Here γ, β_3, β_5 are constant. Wang et al. (Wang et al., 2001) measured specific heat of MgB_2 from 2 K to 300 K and showed Sommerfeld constant $\gamma = 0.89 \pm 0.05$ mJ/K^{2}g (2.7 mJ/K^{2}mol). Obviously, the first term is the contribution of normal electrons and is important only at very low temperature. The second term is offered by phonons. The third one is small and influential only at high temperature. At the normal state of MgB_2, electron's term can be ignored.

Then

$$C_V \approx \beta_3 T^3 + \beta_5 T^5 \tag{10}$$

and

$$\alpha = \gamma_G \kappa_T C_V / (3V) \approx \frac{\gamma_G \kappa_T}{3V}(\beta_3 T^3 + \beta_5 T^5). \tag{11}$$

Noticing that the grain radius variation is a small quantity, the temperature dependence of average grain radius, r(T), can be derived.

$$\frac{1}{r}\frac{\partial r}{\partial T} \approx \frac{\gamma_G \kappa_T}{3V}(\beta_3 T^3 + \beta_5 T^5) \tag{12}$$

$$r(T) \approx r_0 \left[1 + \frac{\gamma_G \kappa_T}{3V}\left(\frac{1}{4}\beta_3 T^4 + \frac{1}{6}\beta_5 T^6\right)\right] \tag{13}$$

Here ρ_0 is the average radius at 0 K. Thus the volume fraction can be rewritten as,

$$\begin{aligned}\phi(T) &= \frac{4}{3}n\pi r^3(T) \\ &= \frac{4}{3}n\pi r_0^3\left[1 + \frac{\gamma_G \kappa_T}{3V}\left(\frac{1}{4}\beta_3 T^4 + \frac{1}{6}\beta_5 T^6\right)\right]^3 \\ &\approx \phi_0\left[1 + \frac{\gamma_G \kappa_T}{V}\left(\frac{1}{4}\beta_3 T^4 + \frac{1}{6}\beta_5 T^6\right)\right] \\ &\equiv \phi_0(1 + \Delta\phi)\end{aligned} \tag{14}$$

Due to the volume fraction variation is very small ($\Delta\phi \ll 1$), the conductivity approximation of SP model is modified.

$$\begin{aligned}\sigma_m^{SPT} &= (\phi_0 - \phi_c)^\mu \sigma_i\left(1 + \frac{\Delta\phi}{\phi_0 - \phi_c}\right)^\mu \\ &\approx (\phi_0 - \phi_c)^\mu \sigma_i(T)\left[1 + \frac{\mu\gamma_G \kappa_T / V}{\phi_0 - \phi_c}\left(\frac{1}{4}\beta_3 T^4 + \frac{1}{6}\beta_5 T^6\right)\right]\end{aligned} \tag{15}$$

We name this expression conductivity approximation of statistical percolation model with temperature (SPT) (Zhang et al., 2010) for a metal-insulator composite. Considering the electrical resistivity of normal-state MgB_2, we have resistivity expression of MgB_2-MgO composite as a function of temperature.

$$\rho_m^{SPT} \approx (\phi_0 - \phi_c)^{-\mu}\left(\rho_{i0} + bT^n\right)\left[1 - \frac{\mu\gamma_G \kappa_T / V}{\phi_0 - \phi_c}\left(\frac{1}{4}\beta_3 T^4 + \frac{1}{6}\beta_5 T^6\right)\right] \tag{16}$$

If we define,

$$\begin{cases} \rho_0 = (\phi_0 - \phi_c)^{-\mu} \rho_{i0} \\ \alpha_n = (\phi_0 - \phi_c)^{-\mu} b \\ \alpha_e = -\dfrac{(\phi_0 - \phi_c)^{-\mu} \rho_{i0}}{4V(\phi_0 - \phi_c)} \mu \gamma_G \kappa_T \beta_3 \end{cases} \quad (17)$$

Then the temperature dependence of resistivity of the superconducting MgB_2-MgO composite has a simple power-law expression as,

$$\rho_m^{SPT} = \rho_0 + \alpha_n T^n + \alpha_e T^4 + \alpha_c T^6 \quad (18)$$

Where ρ_0 relates to the residual resistivity of composite, $\alpha_c T^6$ is a small correction term for the high-power terms of expression (18) and α_c is called as the correction parameter. Fig. 11 shows the fitting resistance vs. temperature of MgB_2 composite with the above expression. Its inset shows that the optimal exponent, n=2.3, which is well consistent with one in the resistivity expression for our MgB_2 multicrystal samples. The coefficient of determination (COD), R-square (R^2), is higher than 0.99996 and the reduced chi-square value, χ^2/DoF, is low to 3.83×10^{-7}. Therefore, the SPT approximation can picture well the conductivity of the superconducting MgB_2-MgO composite at its normal state. It will also be a proper conductivity expression for a metal-insulator composite in which the grain size of metal phase is far larger than the insulator.

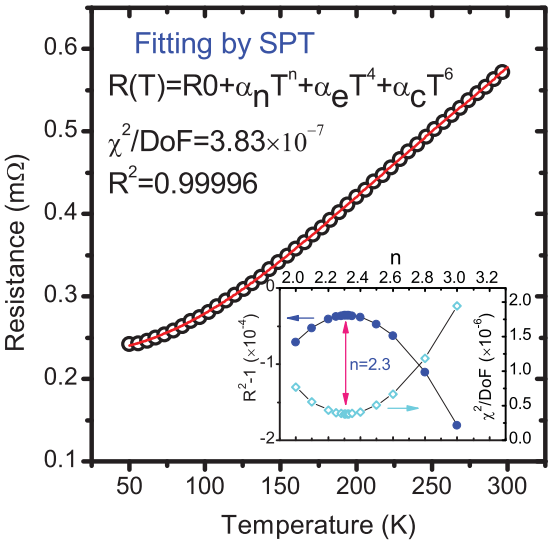

Fig. 11. Fitting the resistance-temperature data of superconducting MgB_2-MgO composite from 50 K to 300 K by the SPT approximation. Solid circle symbols refer to experimental values and the solid line refers to the fitting result. The inset is the fitting R-square and χ^2/DoF at n range from 2.0 to 2.4. The maximum R-square and minimum of χ^2/DoF were obtained at n=2.3 (Zhang et al., 2010).

4. Applications of superconducting MgB_2 composite

The fault current limiter (FCL) is an important components in the electric power system for running safely and stably. In general, it can be performed by power-electronic circuits or positive temperature coefficient (PTC) thermistors. But for a large current or fast response system, the superconducting fault current limiter (SFCL) is the best choice. A composite superconductor is more attractive than a pure-phase superconductor for the application of SFCL because of the broadly current-carrying capacity and mechanical performance by doping. Several superconducting composites have the so-called history effect (HE) in the current-voltage (IV) sweep curve. Using the history effect, a resistive type SFCL (RSFCL) can be easily realized by superconducting composites. HE refers to that the critical current density (j_c) of a superconductor has different values detected in a current sweeping cycle or magnetic field cycle. Fig. 12 shows the current-voltage characteristics of the MgB_2-MgO composite. An anticlockwise HE is observed obviously in the IV curve with two critical currents, I_{c+} = 220 mA and I_{c-}=180 mA.

The HE of the superconducting MgB_2-MgO composite can be understood using the Stewart-McCumber (SM) model for Josephson junctions. Using the history effect, a resistive type SFCL may be designed as shown in Fig. 13. Normally, system is working at a current far lower than the low critical current (I_{c-}) at the superconductive state. When a fault occurs then the transport current increases to exceed the up critical current (I_{c+}), the superconducting MgB_2-MgO composite becomes a normal conductor with a high resistance (R_{RSFCL}). The R_{RSFCL} will restrain the transport current to a limit value. After the system is recovering, the line current decreases to be lower than I_{c-} and the SFCL return to work at the superconductive state then the current is normal.

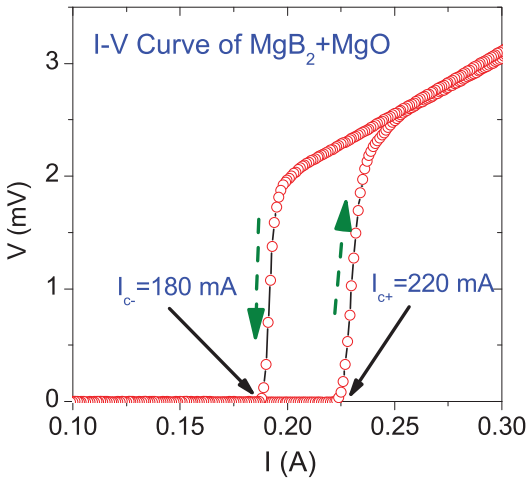

Fig. 12. The current-voltage characteristics of the MgB_2-MgO composite. The current sweeps from 0 mA to 400 mA by a step of 1 mA per 0.1 S, then returns from 400 mA to 0 mA by the same step.

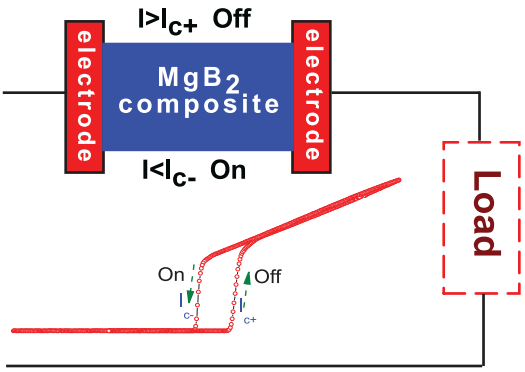

Fig. 13. Diagram for realizing the resistive type SFCL by the superconducting MgB_2-MgO composite.

5. Conclusions

In summary, this chapter introduce a composite superconductor, MgB_2-MgO, which was prepared by a solid-state replacement reaction and vacuum sintering technique. Even the mole fraction of MgO phase was estimated about 75%, the composite exhibited a metallic transport behavior with low resistivity and superconductivity at a high temperature (38.0 K) comparable to a pure-phased MgB_2 sample (39 K). The composite superconductor has the history effect in the current-voltage curve. The results indicate that MgB_2 superconductor can tolerance a high content of insulating contamination and the superconducting MgB_2 MgO composite can be utilized for the superconducting fault current limiter (SFCL). The electrical transport features of the composite are explained by using the statistical percolation model and a conductivity expression with temperature for the metal-insulator MgB_2 composite is given (Zhang et al., 2010),

$$\sigma_m^{SPT} = (\phi_0 - \phi_c)^{\mu}\sigma_i(T)[1 + \frac{\mu\gamma_G\kappa_T / V}{\phi_0 - \phi_c}(\frac{1}{4}\beta_3 T^4 + \frac{1}{6}\beta_5 T^6)].$$

It is considered to be proper for other metal-insulator compounds when the grain size or thermal expansivity of the insulator is far smaller than the metal grain.

6. References

Abeles, B., Pinch, H. L. & Gittleman, J. L. (1975). *Phys. Rev. Lett.* 35: 247.
Ashcroft, N. W. (1968). *Phys. Rev. Lett.* 21: 1748.
Bednorz, J. G. & Müller, K. A. (1986). *Z. Phys. B* 64: 189.
Buzea, C. & Yamashita, T. (2001). *Supercond. Sci. Technol.* 14: R115.
Eom, C. B., Lee, M. K., Choi, J. H., Belenky, L. J., Song, X., Cooley, L. D., Naus, M. T., Patnaik, S., Jiang, J., Rikel, M., Polyanskii, A., Gurevich, A., Cai, X. Y., Bu, S. D., Babcock, S. E., Hellstrom, E. E., Larbalestier, D. C., Rogado, N., Regan, K. A., Hayward, M. A., He, T., Slusky, J. S., Inumaru, K., Haas, M. K. & Cava, R. J. (2001). *Nature* 411: 558.

Gao, Z., Ma, Y., Zhang, X., Wang, D., Wang, J., Awaji, S., Watanabe, K. & Liu, B. (2008). *Supercond. Sci. Technol.* 21: 105020.
Gillijns, W., Aladyshkin, A. Y., Silhanek, A. V. & Moshchalkov, V. V. (2007). *Phys. Rev. B* 76: 060503(R).
John, S. & Lunbensky, T. C. (1985). *Phys. Rev. Lett.* 55: 1014.
John, S. & Lunbensky, T. C. (1986). *Phys. Rev. B* 34: 4815.
Jorgensen, J. D., Hinks, D. G. & Short, S. (2001). *Phys. Rev. B* 63: 224522.
Kambara, M., Babu, N. H., Sadki, E. S., Cooper, J. R., Minami, H., Cardwell, D. A., Campbell, A. M. & Inoue, I. H. (2001). *Supercond. Sci. Technol.* 14: L5.
Kamihara, Y., Hiramatsu, H., Hirano, M., Kawamura, R., Yanagi, H., Kamiya, T. & Hosono, H. (2006). *J. Am. Chem. Soc.* 128: 10012.
Kamihara, Y., Watanabe, T., Hirano, M. & Hosono, H. (2008). *J. Am. Chem. Soc.* 130: 3296.
Kirkpatrick, S. (1973). *Rev. Mod. Phys.* 45: 574.
Larbalestier, D. C., Cooley, L. D., Rikel, M., Polyanskii, A. A., Jiang, J., Patnaik, S., Cai, X. Y., Feldmann, D. M., Gurevich, A., Squitieri, A. A., Naus, M. T., Eom, C. B., Hellstrom, E. E., Cava, R. J., Regan, K. A., Rogado, N., Hayward, M. A., He, T., Slusky, J. S., Khalifah, P., Inumaru, K. & Haas, M. (2001). *Nature* 410: 186.
li Huang, S., Dew-Hughes, D., Zheng, D. N. & Jenkins, R. (1996). *Supercond. Sci. Technol.* 9: 368.
Liao, X. Z., Serquis, A., Zhu, Y. T., Huang, J. Y., Civale, L., Peterson, D. E., Mueller, F. M. & Xu, H. F. (2003). *J. Appl. Phys.* 93: 6208.
Lortz, R., Meingast, C., Ernst, E., Renker, B., Lawrie, D. D. & Frank, J. P. (2003). *J. Low Temp. Phys.* 131: 1101.
Lux, F. (1993). *J. Materials Science* 28: 285.
Ma, Y., Zhang, X., Nishijima, G., Watanabe, K., Awaji, S. & Bai, X. (2006). *App. Phys. Lett.* 88: 072502.
Mamalis, A. G., Ovchinnikov, S. G., Petrov, M. I., Balaev, D. A., Shaihutdinov, K. A., Gohfeld, D. M., Kharlamova, S. A. & Vottea, I. N. (2001). *Physica C* 364-365: 174.
Matsuda, K., Nishimura, K., Ikeno, S., Mori, K., Aoyama, S., Yabumoto, Y., Hishinuma, Y., Mullerova, I., Frank, L., Yurchenko, V. V. & Johansen, T. H. (2008). *J. Phys.: Conference Series* 97: 012230.
Matsumoto, K., Takewaki, H., Tanaka, Y., Miura, O., Yamafuji, K., Funaki, K., Iwakuma, M. & Matsushita, T. (1994). *Appl. Phys. Lett.* 64: 115.
McLachlan, D. S., Chiteme, C., Heiss, W. D. &Wu, J. (2003). *Physica B* 338: 261.
Nagamatsu, J., Nakagawa, N., Muranaka, T., Zenitani, Y. & Akimitsu, J. (2001). *Nature* 410: 63.
Nan, C.-W. (1993). *Progr. Mat. Sci.* 37: 1.
Neumeier, J. J., Tomita, T., Debessai, M., Schilling, J. S., Barnes, P.W., Hinks, D. G. & Jorgensen, J. D. (2005). *Phys. Rev. B* 72: 220505(R).
Petrov, M. I., Balaev, D. A., Gohfeld, D. M., Ospishchev, S. V., Shaihudtinov, K. A. & Aleksandrov, K. S. (1999). Physica *C* 314: 51.
Przybylski, K., Stobierski, L., Chmist, J. & Kolodziejczyk, A. (2003). *Physica C* 387: 148.
Ren, Z. A., Lu,W., Yang, J., Yi,W., Li, X. L. S. Z. C., Che, G. C., Dong, X. L., Sun, L. L., Zhou, F. & Zhao, Z. X. (2008). *Chin Phys. Lett.* 25: 2215.
Rowell, J. M. (2003). *Supercond. Sci. Technol.* 16: R17.
Shih,W. Y., Ebner, C. & Stroud, D. (1984). *Phys. Rev. B* 30: 134.

Siemons,W., Steiner, M. A., Koster, G., Blank, D. H. A., Beasley, M. R. & Kapitulnik, A. (2008). *Phys. Rev. B* 77: 174506.

Takahashi, H., Igawa, K., Arii, K., Kamihara, Y. & andH. Hosono, M. H. (2008). *Nature* 453: 376.

Varshney, D. (2006). *Supercond. Sci. Technol.* 19: 685.

Wang, X. L., Soltanian, S., James, M., Qin, M. J., Horvat, J., Yao, Q. W., Liu, H. K. & Dou, S. X. (2004). *Physica C* 408C410: 63.

Wang, Y., Plackowski, T. & Junod, A. (2001). *Physica C* 355: 179.

Xi, X. X. (2008). *Rep. Prog. Phys.* 71: 116501.

Xi, X. X., Pogrebnyakov, A. V., Xu, S. Y., Chen, K., Cui, Y., Maertz, E. C., Zhuang, C. G., Li, Q., Lamborn, D. R., Redwing, J. M., Liu, Z. K., Soukiassian, A., Schlom, D. G., Weng, X. J., Dickey, E. C., Chen, Y. B., Tian, W., Pan, X. Q., Cybart, S. A. & Dynes, R. C. (2007). *Physica C* 456: 22.

Xue, Y., Asada, S., Hosomichi, A., Naher, S., Xue, J., Kaneko, H., Suzuki, H., Muranaka, T. & Akimitsu, J. (2005). *J. Low Temp. Phys.* 138: 1105.

Zallen, R. (1983). *The physics of amorphous solids*, Wley, New York.

Zeng, X. H., Sukiasyan, A., Xi, X. X., Hu, Y. F.,Wertz, E., Li, Q., Tian,W., Sun, H. P., Pan, X. Q., Lettieri, J., Schlom, D. G., Brubaker, C. O., Liu, Z.-K. & Li, Q. (2001). *Appl. Phys. Lett.* 79: 1840.

Zhang, Y. B., Zeng, M., Gao, Z. S., Liu, J., Zhu, H. M. & Zhou, S. P. (2009). *J. Supercond. Nov. Magn.* 22: 729.

Zhang, Y. B., Zhou, D. F., Lv, Z. X., Deng, Z. Y., Cai, C. B. & Zhou, S. P. (2010). *J. Appl. Phys.* 107: 123907.

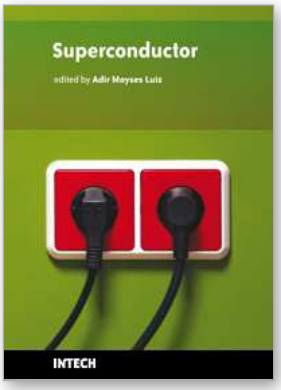

Superconductor

Edited by Doctor Adir Moyses Luiz

ISBN 978-953-307-107-7
Hard cover, 344 pages
Publisher Sciyo
Published online 18, August, 2010
Published in print edition August, 2010

This book contains a collection of works intended to study theoretical and experimental aspects of superconductivity. Here you will find interesting reports on low-Tc superconductors (materials with Tc< 30 K), as well as a great number of researches on high-Tc superconductors (materials with Tc> 30 K). Certainly this book will be useful to encourage further experimental and theoretical researches in superconducting materials.

How to reference

In order to correctly reference this scholarly work, feel free to copy and paste the following:

YiBing Zhang and Shiping Zhou (2010). MgB2-MgO Compound Superconductor, Superconductor, Doctor Adir Moyses Luiz (Ed.), ISBN: 978-953-307-107-7, InTech, Available from: http://www.intechopen.com/books/superconductor/mgb2-mgo-compound-superconductor

INTECH
open science | open minds

InTech Europe
University Campus STeP Ri
Slavka Krautzeka 83/A
51000 Rijeka, Croatia
Phone: +385 (51) 770 447
Fax: +385 (51) 686 166
www.intechopen.com

InTech China
Unit 405, Office Block, Hotel Equatorial Shanghai
No.65, Yan An Road (West), Shanghai, 200040, China
中国上海市延安西路65号上海国际贵都大饭店办公楼405单元
Phone: +86-21-62489820
Fax: +86-21-62489821